Annals of Botany **114**: 1627–1635, 2014
doi:10.1093/aob/mcu180, available online at www.aob.oxfordjournals.org

ANNALS OF BOTANY Founded 1887

Plant material features responsible for bamboo's excellent mechanical performance: a comparison of tensile properties of bamboo and spruce at the tissue, fibre and cell wall levels

Xiaoqing Wang[1,2,3], Tobias Keplinger[1,2], Notburga Gierlinger[1,2] and Ingo Burgert[1,2,*]

[1]*Institute for Building Materials, ETH-Swiss Federal Institute of Technology Zurich, CH-8093 Zurich, Switzerland,* [2]*Applied Wood Materials Laboratory, EMPA-Swiss Federal Laboratories for Materials Science and Technology, CH-8600 Dübendorf, Switzerland and* [3]*Research Institute of Wood Industry, Chinese Academy of Forestry, Beijing 100091, China*
** For correspondence. E-mail iburgert@ethz.ch*

Received: 3 April 2014 Returned for revision: 1 July 2014 Accepted: 25 July 2014 Published electronically: 1 September 2014

• **Background and Aims** Bamboo is well known for its fast growth and excellent mechanical performance, but the underlying relationships between its structure and properties are only partially known. Since it lacks secondary thickening, bamboo cannot use adaptive growth in the same way as a tree would in order to modify the geometry of the stem and increase its moment of inertia to cope with bending stresses caused by wind loads. Consequently, mechanical adaptation can only be achieved at the tissue level, and this study aims to examine how this is achieved by comparison with a softwood tree species at the tissue, fibre and cell wall levels.
• **Methods** The mechanical properties of single fibres and tissue slices of stems of mature moso bamboo (*Phyllostachys pubescens*) and spruce (*Picea abies*) latewood were investigated in microtensile tests. Cell parameters, cellulose microfibril angles and chemical composition were determined using light and electron microscopy, wide-angle X-ray scattering and confocal Raman microscopy.
• **Key Results** Pronounced differences in tensile stiffness and strength were found at the tissue and fibre levels, but not at the cell wall level. Thus, under tensile loads, the differing wall structures of bamboo (multilayered) and spruce (sandwich-like) appear to be of minor relevance.
• **Conclusions** The superior tensile properties of bamboo fibres and fibre bundles are mainly a result of amplified cell wall formation, leading to a densely packed tissue, rather than being based on specific cell wall properties. The material optimization towards extremely compact fibres with a multi-lamellar cell wall in bamboo might be a result of a plant growth strategy that compensates for the lack of secondary thickening growth at the tissue level, which is not only favourable for the biomechanics of the plant but is also increasingly utilized in terms of engineering products made from bamboo culms.

Key words: Bamboo, *Phyllostachys pubescens*, spruce, *Picea abies*, stem biomechanics, plant cell wall, mechanical adaptation, microfibril angle, Raman imaging, tensile stiffness.

INTRODUCTION

Plants have adopted different growth strategies to form numerous types of stem structure with specific functional anatomy and excellent mechanical properties to fulfil a multiplicity of functions, such as mechanical support and water transport to ensure survival and competitiveness in their respective habitats (Speck and Burgert, 2011; Niklas and Spatz, 2012). The monocotyledonous bamboos grow fast in length but do not show secondary thickening to add cells to their periphery, and the final diameter of the stem is determined in the initial growth phase, which results in a slender stem with a hollow structure. In contrast, softwood and hardwood trees can grow not only in length but also in width due to the presence of a vascular cambium. This growth strategy offers a tree much higher capacity to adapt the geometry of the stem and increase its moment of inertia to cope with bending stresses caused by wind loads. As a consequence of these diverging growth constraints, the mechanical exposure of the tissues of bamboos and trees is quite different, which most probably has resulted in different adaptation strategies at the plant material level (Eder *et al.*, 2009).

Comparing tree (in this case a gymnosperm) and bamboo tissue structure at different levels of hierarchy reveals the general differences in plant material design. A spruce tree trunk possesses the typical growth ring structure, consisting of bright regions of earlywood alternating with darker regions of latewood (Fig. 1A). The earlywood is made up of tracheids with large lumina and thin cell walls mainly serving for water transport, while the latewood is composed of tracheids with thick cell walls and small lumina that are favourable for mechanical support. In contrast, bamboos possess numerous vascular bundles, consisting of xylem, phloem and fibre caps, which are embedded in parenchymatous tissues (Fig. 1B). The main function of xylem and phloem is transport of water and nutrients, while the sclerenchymatous fibres caps are the main stiffening elements providing mechanical support for the stem. The distribution of the vascular bundles is not uniform across the stem, exhibiting a marked radial gradient in concentration with densely packed bundles at the stem periphery, where the bending stresses on the stem are highest (Amada *et al.*, 1997).

Structural adaptation is further manifested at the cell and cell wall levels. Wood tracheids die at the end of their differentiation

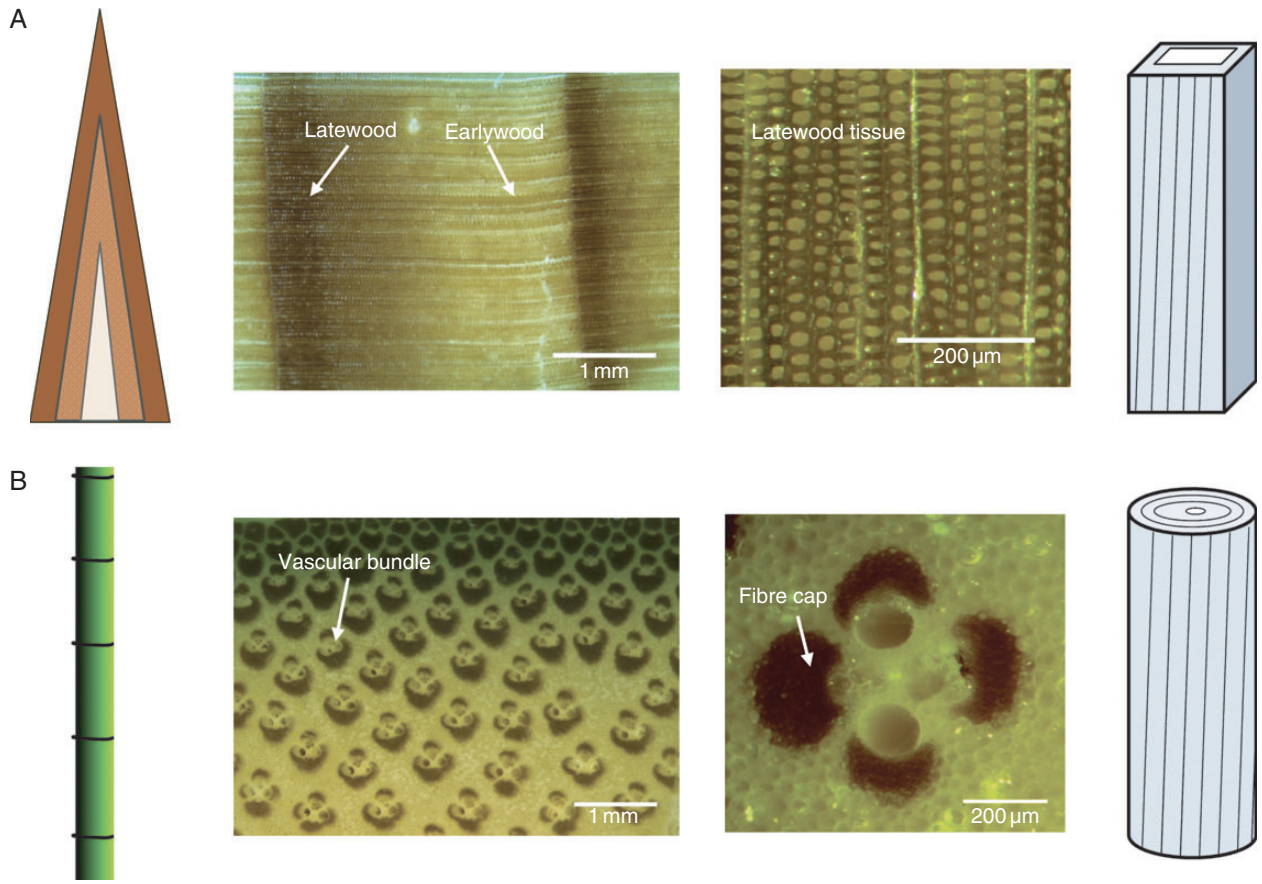

FIG. 1. Different tissue and cell wall structures as a result of the specific growth constraints in (A) spruce (*Picea abies*) and (B) bamboo (*Phyllostachys pubescens*). A conifer stem grows in both height and diameter with a typical growth ring structure and develops tube-shaped fibres (tracheids). By contrast, the monocotyledonous bamboo, lacking secondary thickening, forms a specific stem structure with vascular bundles embedded in parenchymatous tissue, and develops thick-walled fibres.

stage after secondary cell wall formation has been finalized. Hence, the cell wall structure and mechanical properties of tracheids are determined and cannot be further tuned at a later growth phase. The secondary cell wall of wood tracheids usually consists of three layers, with a dominating middle layer (S2), which has a small cellulose microfibril angle, while the outer S1 layer and the inner S3 layer possess higher microfibril angles. In contrast, in monocotyledonous bamboos, both the parenchymatous tissue and the supporting fibres stay alive and are modulated during the entire development of the plant. As the bamboo ages and grows taller, new cell wall layers are formed in the supporting fibres, resulting in increased cell wall thickness, which is accompanied by cell wall lignification (Murphy and Alvin, 1997; Lin *et al.*, 2002; Gritsch *et al.*, 2004; Wang *et al.*, 2012). This progressive deposition of new wall layers in the secondary cell wall leads to a multilayered wall structure of the supporting fibres at maturity, which is in contrast to the sandwich-like wall structure of wood tracheids. This multilayered wall structure is characterized by an alternation of thick layers with low microfibril angles and thin layers with high microfibril angles (MFAs) (Parameswaran and Liese, 1976, 1980; Crow and Murphy, 2000). Furthermore, the degree of lignification varies considerably across the cell wall layers, with much higher lignin content in the thin layers and less lignin in the thick layers (Parameswaran and Liese, 1976).

Since bamboo lacks secondary thickening growth, it cannot grow like a tree to adapt the geometry of the stem and increase its moment of inertia to cope with bending stresses caused by wind loads. As a consequence, mechanical adaptation has to be achieved exclusively at the plant material level, which is likely to be more demanding in terms of plant material mechanics compared with trees. In consequence, it seems reasonable to assume that adaptation at the plant tissue level should have resulted in an optimized tissue with superior material performance. In fact there are various studies that emphasize the excellent mechanical properties of bamboo at all length scales from the entire culm down to fibre bundles and single sclerenchymatic fibres of the fibre cap (Obataya *et al.*, 2007; Shao *et al.*, 2010; Li and Shen, 2011; Yu *et al.*, 2011) and some even claim outstanding mechanical properties of bamboo fibres that are comparable to those of glass fibres (Okubo *et al.*, 2004; Osorio *et al.*, 2011). However, in view of the above-mentioned considerations on material adaptation, a systematic comparison of bamboo properties with wood properties at the tissue, fibre and cell levels is needed to (1) unravel general differences in material behaviour between wood and bamboo fibres and (2) identify the level of hierarchy at which different adaptation strategies result in deviating property profiles. For this purpose we compared bamboo fibre caps and spruce latewood at the tissue, fibre and cell wall levels by

means of mechanical, structural and chemical characterization techniques.

MATERIALS AND METHODS

Sample preparation

A 4-year-old moso bamboo (*Phyllostachys pubescens*) culm, with a total height of ∼13 m and diameter at breast height of 10·5 cm, was harvested from a local experimental forest in Miaoshanwu Nature Reserve (119°56′–120°02′E, 30°03′–30°06′N), Zhejiang Province, China. Small blocks with the dimensions of 25 mm [longitudinal (L)] × 8 mm [tangential (T)] × 10 mm [radial (R)] were removed from the tenth internode section of the stem and 100-μm-thick slices (LT plane) were cut from the blocks using a rotary microtome to provide fibres and fibre bundles for the microtensile tests. Single fibres were carefully peeled out of the thin slices using very fine tweezers under a light microscope (Burgert *et al.*, 2002). Similarly, fibre bundles ∼100–300 μm in width were mechanically isolated by taking advantage of the weak interfacial adhesion between fibre caps and parenchyma cells. In parallel, 100-μm-thick wood slices (LT plane) were prepared from a normal adult spruce (*Picea abies*) wood block. Only slices of latewood were selected to provide single fibres (tracheids) and tissue foils for the mechanical tests. Single wood fibres were mechanically isolated using the same procedure as described above. Tissue foils were cut from the latewood slices using a sharp razor blade with a sample size comparable to that of the bamboo fibre bundles. All prepared samples were air-dried between two glass slides to avoid twisting prior to mechanical tests. The length of single fibres was measured using a light microscope equipped with a measuring eyepiece.

Microtensile tests

The mechanical properties of the single fibres were tested by using a microtensile testing device equipped with a 500 mN maximum capacity load as described in detail in Burgert *et al.* (2003). For easy handling, the delicate bamboo and wood fibres were fixed in the microtensile apparatus by a pin-hole assembly, with a test span of ∼1 mm. The samples were strained with a displacement rate of 2 μm s^{-1} until failure. In order to achieve sufficiently precise strain measurements, fibre elongation during testing was recorded by video extensometry. For fibre bundle (tissues foil) testing, some modifications were made with respect to the tensile testing device. A load cell with a maximum capacity of 50 N was used due to the expected higher forces required to break the samples, and fibre bundles were clamped by pressure bars instead of the pin-hole assembly described above. The free test length was ∼8 mm and the samples were strained with a displacement rate of 3 μm s^{-1} until failure. All tensile tests were performed in an environment of 20 °C and 50 % relative humidity.

To calculate the ultimate stress and stiffness of the fibres and fibre bundles, both the cell and cell wall cross-sectional areas were determined according to the method described previously (Burgert *et al.*, 2005). Typically, one part of the broken samples was embedded in polyethylene glycol 2000 followed by sectioning with razor blades and rinsing with water. The sectioned surfaces were then observed using an environmental scanning electron microscope (ESEM; FEI Quanta 600) to obtain images for area calculation using the software ImageJ (1.43u).

In total, 16 bamboo fibres and 33 fibre bundles as well as 21 spruce fibres and 45 tissue foils were successfully tested and analysed. Data were graphically represented using box-and-whisker plots to compare the tensile properties of bamboo and spruce fibres (tissues). A non-parametric Mann–Whitney *U*-test was performed to verify statistically significant differences between the groups, using OriginPro 8 SR0 (http://www.originlab.com/).

Wide-angle X-ray scattering experiments

Wide-angle X-ray scattering (WAXS) experiments were performed on the mechanically isolated fibre bundles (tissue foils) to determine the cellulose microfibril angle (MFA) with a Nanostar instrument (Bruker AXS), with a sample–detector distance of 5 cm using Cu Kα radiation (wavelength 0·154 nm). The diffraction patterns were collected with a 2-D position-sensitive (Hi-star) detector for 1 h. Intensity was plotted against the azimuthal angle, and the 002 reflection was used to calculate the MFA according to the method described by Lichtenegger *et al.* (1998). The calculated value represented the average MFA of all fibres present in the sample region hit by the beam.

Raman analysis

For sample preparation, 15-μm-thick cross-sections were cut from bamboo and wood blocks using a rotary microtome (RM 2255; Leica, Germany). The cross-sections were placed on glass slides and wetted with deuterium oxide (D_2O; Aldrich). To avoid evaporation and drying out during measurements, the sections were covered with glass coverslips (0·17 mm thick) and sealed with nail polish. Spectra were acquired with a confocal Raman microscope (InVia; Renishaw, UK) equipped with a motorized xyz stage. To achieve high spatial resolution, a 100 × oil immersion microscope objective [numerical aperture (NA) 1·3; Nikon] and a linearly polarized green laser (λ = 532 nm) was used. The laser was focused with a diffraction-limited spot size of 0·61 × λ/NA onto the samples and the Raman light was detected by an air-cooled charge-coupled device (CCD) camera behind a spectrometer (InVia) with a spectral resolution of 1 cm^{-1}. The laser power on the sample was ∼7 mW.

Wire 3.4 (Renishaw) and CytoSpec (version 2.00.01) software were used for measurement setup as well as image processing and analysis. Chemical images were generated using a sum filter by integrating over defined wavenumber regions in the spectrum. The filter calculated the intensities within the chosen borders and the background was subtracted by taking the baseline from the first to the second border. Sample areas of 45 × 45 μm^2 in bamboo fibre caps and 65 × 42 μm^2 in spruce latewood region were selected for Raman mapping at 0·3-μm step size with an integration time of 0·15 s. The chemical images enabled distinction between cell wall regions differing in chemical composition and/or cellulose orientation with the colour scale bar based on variation of Raman intensity (CCD counts). Average spectra from these regions of interest were extracted and baseline corrected for detailed analysis.

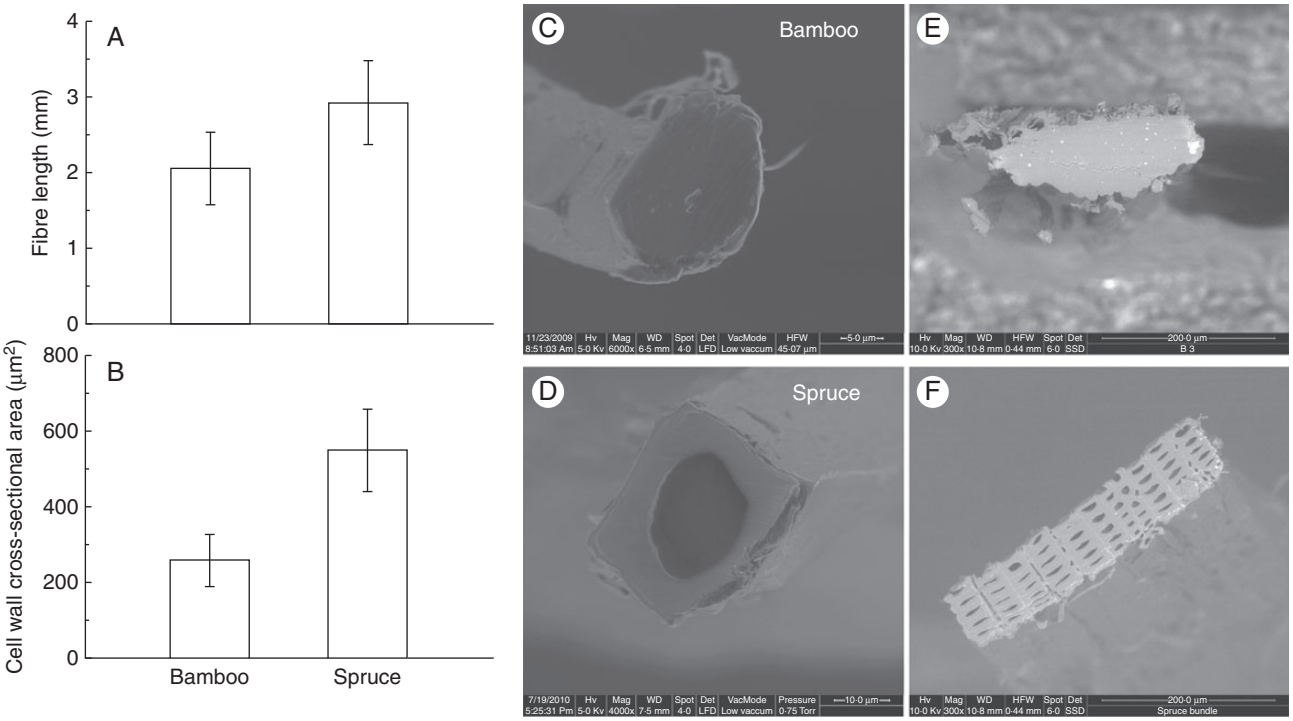

FIG. 2. (A) Fibre length and (B) cell wall cross-sectional area of bamboo fibre and spruce latewood tracheids (data are mean ± s.d.). Scanning electron microscopy images of cross-sections of (C, D) single fibres and (E, F) fibre bundles of bamboo (C, E) and spruce latewood (D, F) cut using razor blades.

RESULTS

Tissue and fibre morphology

The single fibres obtained by mechanical isolation retained their original shape without altering cell wall structure, which is of great importance when investigating structure–property relationships at the individual cell level. Spruce latewood tracheids and bamboo fibres showed clear differences in terms of cell shape and cell wall features. Bamboo fibres were approximately one-third shorter in length compared with the wood tracheids (Fig. 2A). They exhibited a smaller diameter (Fig. 2C and D) with a cell wall cross-sectional area only half of that of wood tracheids (Fig. 2B). The observed latewood tracheids had the typical appearance, with a nearly rectangular or hexagonal cell shape with a thick cell wall and a small lumen. The bamboo fibres exhibited an essentially round shape in cross-section, appearing like a solid tube with a negligible lumen. Figure 2 (E, F) shows the tissue samples that had been mechanically tested. Because there was almost no lumen the bamboo fibre bundles appeared to be more densely packed in comparison with the spruce latewood.

Cell wall analysis

The WAXS patterns of bamboo fibre bundles indicated a strong scattering signal that originated mainly from the axially oriented cellulose microfibrils of the thick layers of the multilayered secondary walls of fibres, giving an MFA of $\sim 9^{\circ}$ with respect to the cell axis. Consistently, a rather small MFA of $\sim 10^{\circ}$ was calculated from the WAXS patterns for the S2 layer of spruce latewood (data not shown).

Raman imaging was conducted to reveal further structure details and cell wall chemistry with resolution at the micro-level. False-colour images were generated by integrating over the intensity of defined Raman spectral bands, showing the distribution of cellulose and lignin in the cell walls. The spatial distribution of cellulose was visualized (Fig. 3A, B) based on the spectral band at 377 cm^{-1} due to C–C–C ring deformation vibration (Gierlinger and Schwanninger, 2007). The spectroscopic images clearly showed higher cellulose content in the secondary cell wall than in the compound middle lamella (CML) and the cell corner (CC) for both cell types. However, due to the uneven sample surface or changes in laser intensity during spectral recording, non-homogeneous distribution of cellulose in the cell walls was observed. By integrating over the strong bands around 1600 cm^{-1}, the spatial distribution of lignin was visualized (Fig. 3C, D). For both cell types, the CC and CML regions were heavily lignified compared with the secondary cell wall. Compared with wood tracheids, the degree of lignification in the CC and CML of bamboo fibres seemed to be much higher.

Raman mapping also allowed visualization of the orientation of cellulose microfibrils within the plant cell walls and added further information to the WAXS analysis (Fig. 4). By examining the cellulose-orientation-sensitive bands at 1092 cm^{-1} due to C–O–C stretching of cellulose, the cell wall regions parallel to the laser direction with high cellulose MFAs could be resolved (Gierlinger *et al.*, 2012). In spruce the S1 layer of the secondary wall of wood tracheids was revealed, while in bamboo also the thin layers (100–200 nm in width) across the cell wall were clearly visualized. On the other hand, by integration over the C–H stretching band of cellulose at 2892 cm^{-1} accentuating

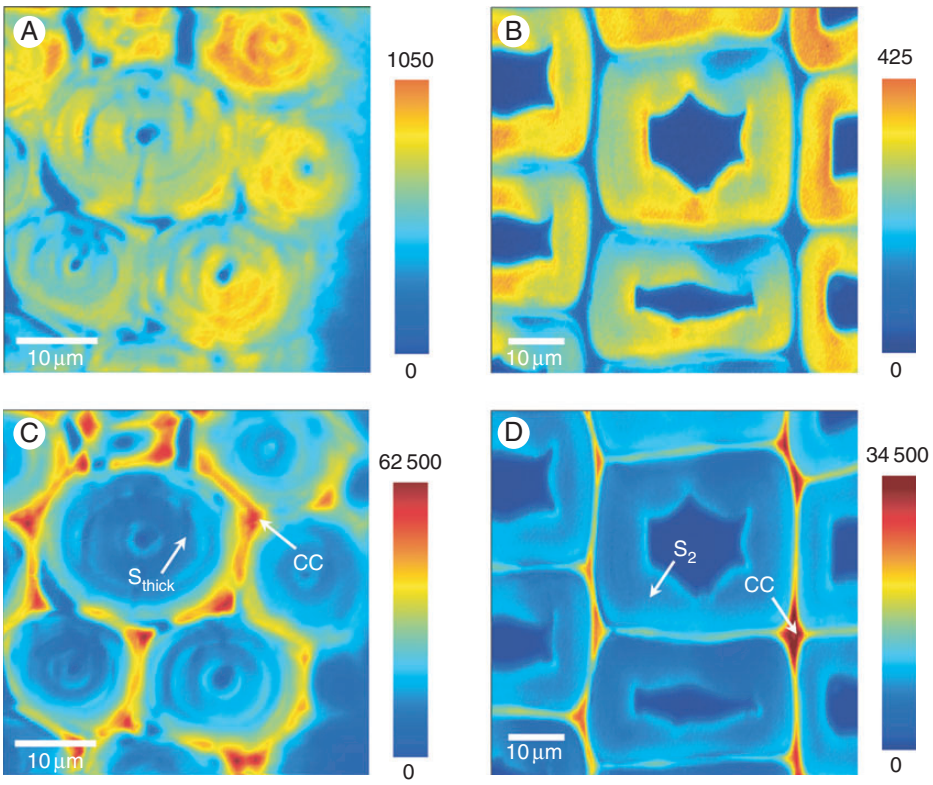

FIG. 3. Raman spectroscopic images showing distribution of cellulose and lignin in cell walls of bamboo fibres and spruce latewood (scales show number of counts). (A) Distribution of cellulose in bamboo by integrating from 335 to 400 cm^{-1}, (B) cellulose in spruce, integrating from 365 to 400 cm^{-1}, (C) lignin (coupled with phenolic acids) in bamboo, integrating from 1525 to 1750 cm^{-1} and (D) lignin in spruce, integrating from 1525 to 1715 cm^{-1} (intensity scales show number of CCD counts).

cellulose orientation in the fibre direction (Gierlinger and Schwanninger, 2006), the thick S2 layer of the secondary wall of wood tracheids was highlighted, while the thick layers could be differentiated from the thin layers in the secondary wall of bamboo fibres. Thus, by Raman mapping, the fine multilayered wall structure with alternating thick and thin layers of differing microfibril angles could be visualized, which is in accordance with the bamboo wall structure reported previously (Parameswaran and Liese, 1976).

Furthermore, average spectra were extracted from the secondary cell wall and the CC of both cell types for a detailed analysis with regard to lignin content and structure. The spectra of the CCs of both cell types showed strong aryl ring stretching of lignin at ~1600 cm^{-1}, in contrast to the much weaker lignin signals in the spectra of the secondary cell walls (Fig. 5). The lignin-specific peaks revealed different intensities and band shapes, reflecting pronounced differences in lignin structure in the CCs of bamboo and wood cells. In the CC spectrum of wood, the aryl stretching vibration at 1597 cm^{-1} was accompanied by a shoulder peak at 1654 cm^{-1}, assigned to coniferyl alcohol and coniferaldehyde (Agarwal, 1999). By contrast, in the spectrum of bamboo the very strong aryl ring stretching at 1600 cm^{-1} was a clear doublet with a second peak at 1631 cm^{-1}, accompanied by a weak peak at 1683 cm^{-1}. This doublet peak, as well as the band at 1173 cm^{-1}, indicated clearly the presence of hydroxycinnamic acids (ferulic and *p*-coumaric acids) in bamboo cell walls (Takei *et al.*, 1995; Ram *et al.*, 2003). The CC spectrum of wood showed characteristic peaks of guaiacyl (G) and syringyl (S) units of lignin at 1272 and 1333 cm^{-1}, respectively (Agarwal and Ralph, 1997; Perera *et al.*, 2012), whereas the peaks of G and S units shifted slightly in the spectrum of bamboo, in which an additional peak appeared at ~1206 cm^{-1}, indicating the presence of *p*-hydroxyphenyl (H) units (Sun *et al.*, 2012). However, it should be noted that hydroxycinnamic acids also make considerable contributions to these peaks of lignin structural units. Finally it can be concluded that compared with spruce wood tracheids, a large amount of hydroxycinnamic acids is located in the CCs of bamboo fibres.

Mechanical tests

The mechanically isolated fibre bundles (tissue foils) of bamboo and spruce latewood were tested in a microtensile testing stage, and the calculated stress–strain curves of the samples are shown in Fig. 6. Both bamboo fibre bundles and latewood samples exhibited linear–elastic deformation behaviour, partly with some larger deformations at high strain levels close to failure, which generally indicated a typical rather brittle and stiff material behaviour (Fig. 6A, B). For comparison of the tensile properties in both tissue types, the modulus of elasticity and ultimate stress were calculated on the basis of the sample cross-section (Fig. 6C, D). The bamboo fibre bundles showed a mean modulus of elasticity of ~25 GPa and a mean ultimate stress of ~646 MPa. These values are comparable to the tensile properties of bamboo vascular bundles reported previously (Li and Shen, 2011). For spruce latewood tissues, the tensile

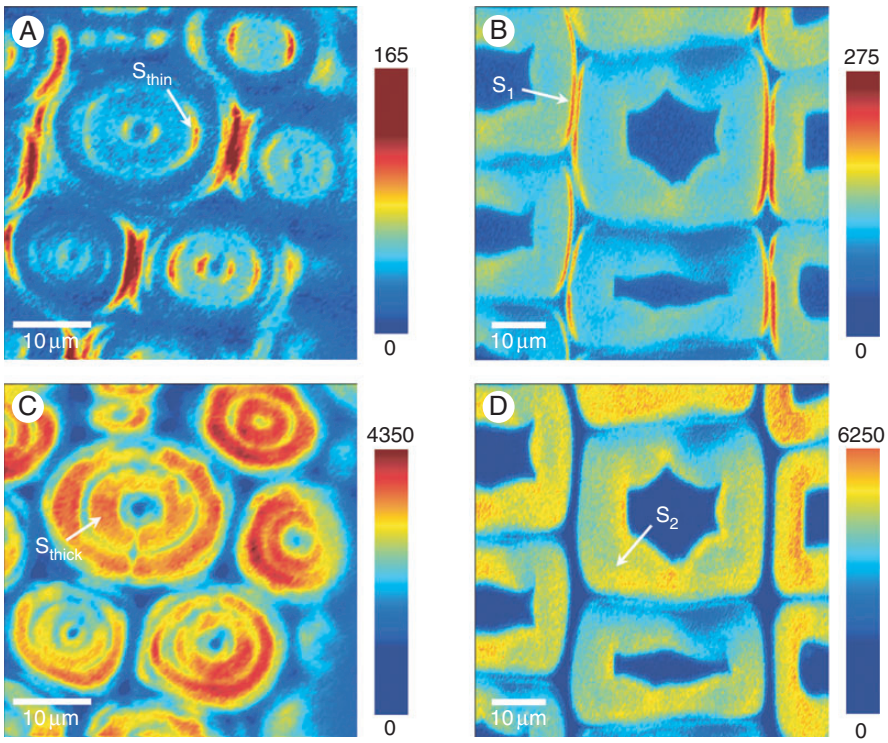

FIG. 4. Raman spectroscopic images showing the orientation of cellulose microfibrils in cell walls (scales show number of counts). (A) Images integrated on the basis of the C–O–C stretching band of cellulose at 1092 cm^{-1} (1064–1103 cm^{-1}) visualizing the thin wall layers (S_{thin}) of bamboo fibres, and (B) from 1075 to 1105 cm^{-1} visualizing the S1 layer of the wood cell wall. (C) Images integrated based on the C–H stretching band of cellulose at 2894 cm^{-1} (2790–2926 cm^{-1}) accentuating the thick wall layers (S_{thick}) of bamboo fibres, with cellulose oriented in the fibre direction, and (D) from 2800 to 2930 cm^{-1}, highlighting the S2 layer of the wood cell wall (intensity scales show number of CCD counts).

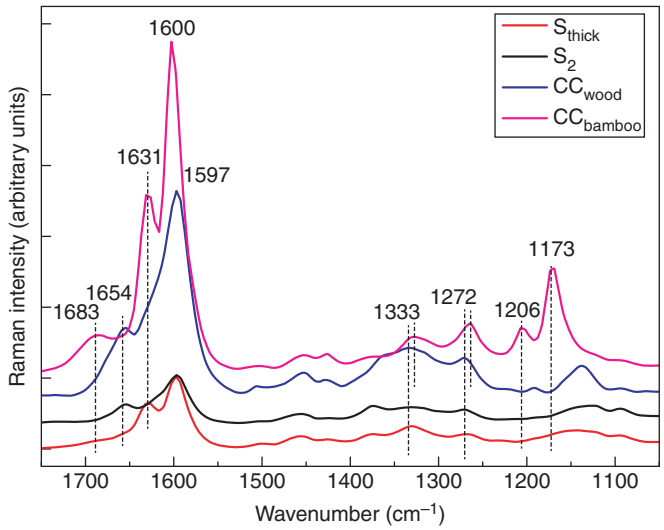

FIG. 5. Average spectra extracted from the secondary wall (S) and cell corner (CC) of bamboo fibres and wood tracheids as indicated in Fig. 3C, D.

properties were considerably lower than the corresponding properties of bamboo fibre bundles. The mean modulus of elasticity was ~17 GPa and the mean ultimate stress was ~364 MPa.

In order to monitor the mechanical properties of the fibres and to distinguish between the mechanical response of the cell wall and contributions from cell–cell interactions in the tissues, the mechanical properties of individual fibres were also determined. The stress–strain curves of the bamboo fibres and spruce latewood tracheids are presented in Fig. 7A and B. Both fibre types exhibited linear deformation behaviour until failure, without an obvious yield point, which resembled the mechanical behaviour of the tissues. The cell and cell wall cross-sections were considered when calculating the modulus of elasticity and ultimate stress, respectively. As bamboo fibres possess an almost negligible lumen, fibre and cell wall properties are not distinguished for bamboo. At the fibre level the mean tensile modulus and mean ultimate stress were markedly higher in bamboo fibres than in wood tracheids. However, when the cell wall area was used for the calculation of stresses, bamboo and spruce had almost the same properties (Fig. 7C, D). The bamboo fibre cell walls had a mean tensile modulus of ~28 GPa and a mean ultimate stress of ~985 MPa, whereas the spruce latewood cell walls had a mean tensile modulus of ~25 GPa and a mean ultimate stress of ~918 MPa; no statistically significant differences were found based on the Mann–Whitney *U*-test ($P > 0{\cdot}05$).

Figure 8 shows the comparison of mechanical properties by compiling typical stress–strain curves of fibres and tissues for bamboo and spruce latewood, calculated on the basis of cell wall cross-sections for better comparability. For both species, the tissue slices exhibited tensile stiffness comparable to that of single fibres, but they failed at a much smaller strain upon stretching compared with single fibres, resulting in a much lower tensile strength.

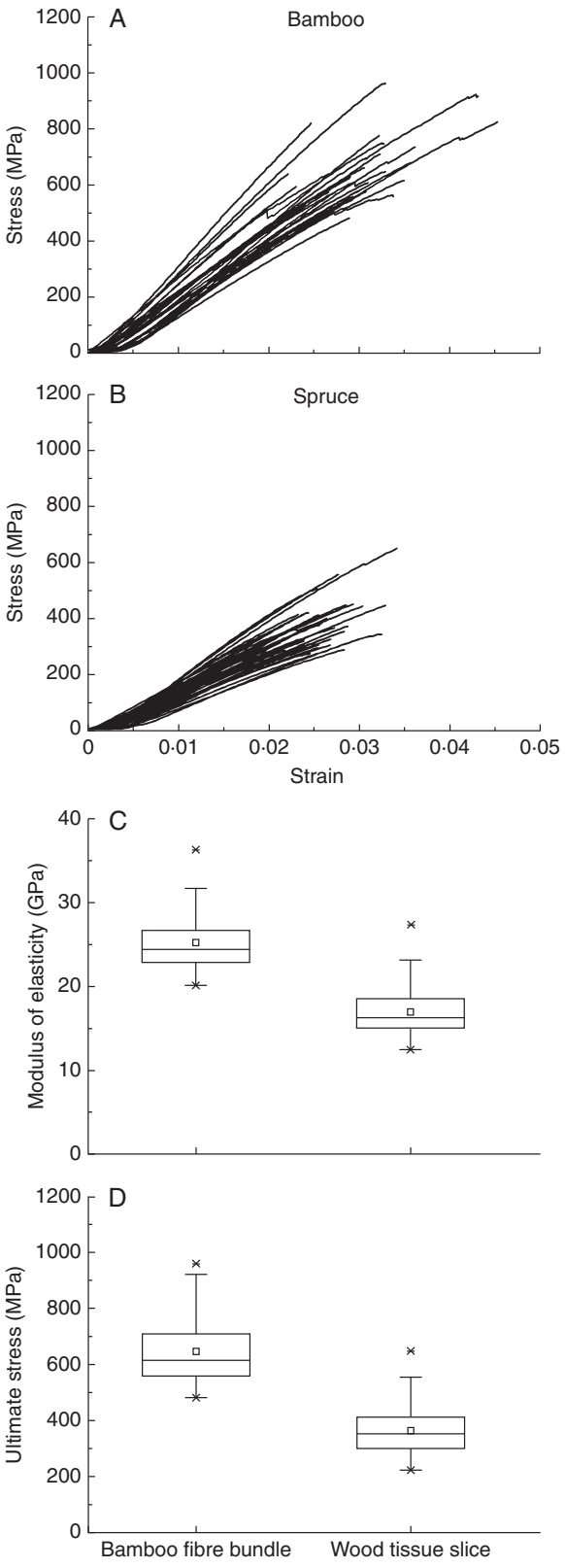

FIG. 6. Stress–strain curves for (A) fibre bundles (tissue) of bamboo and (B) spruce latewood examined in tensile tests. Box-and-whisker plots of (C) modulus of elasticity and (D) ultimate stress were calculated on the basis of cell cross-sections.

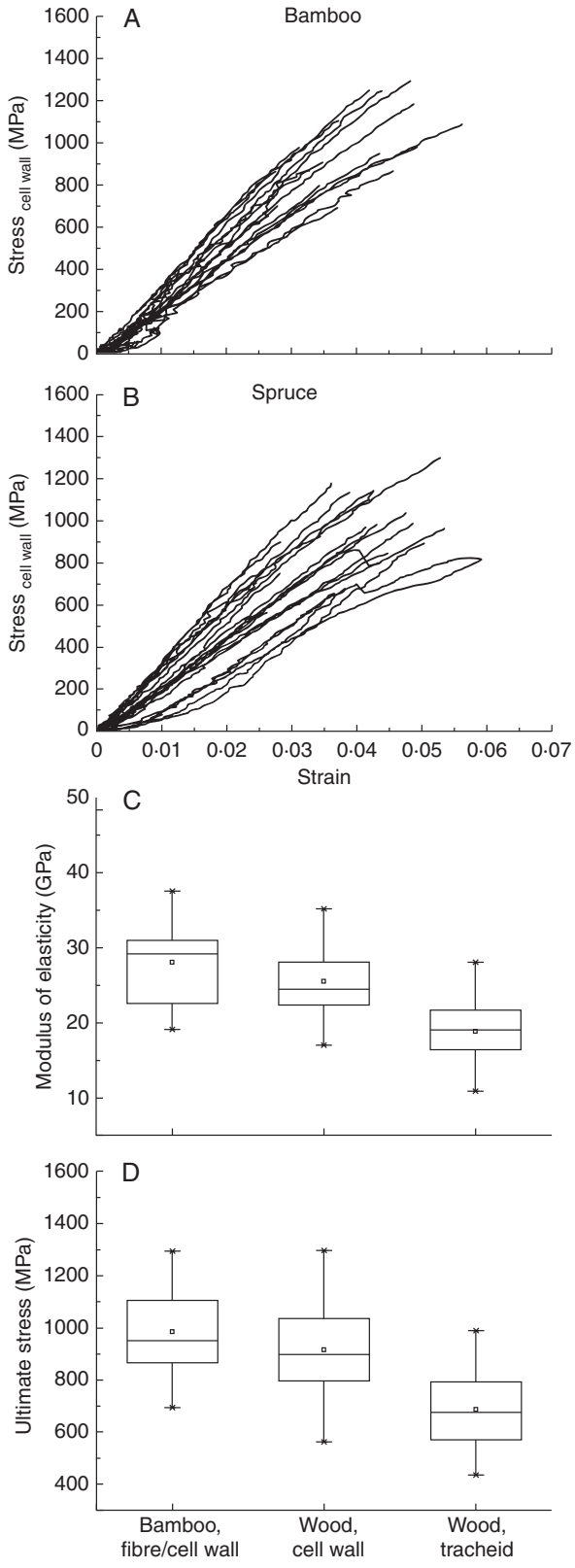

FIG. 7. Stress–strain curves of (A) single fibres of bamboo and (B) spruce latewood examined in tensile tests. Box-and-whisker plots of (C) modulus of elasticity and (D) ultimate stress were calculated on the basis of cell and cell wall cross-sections.

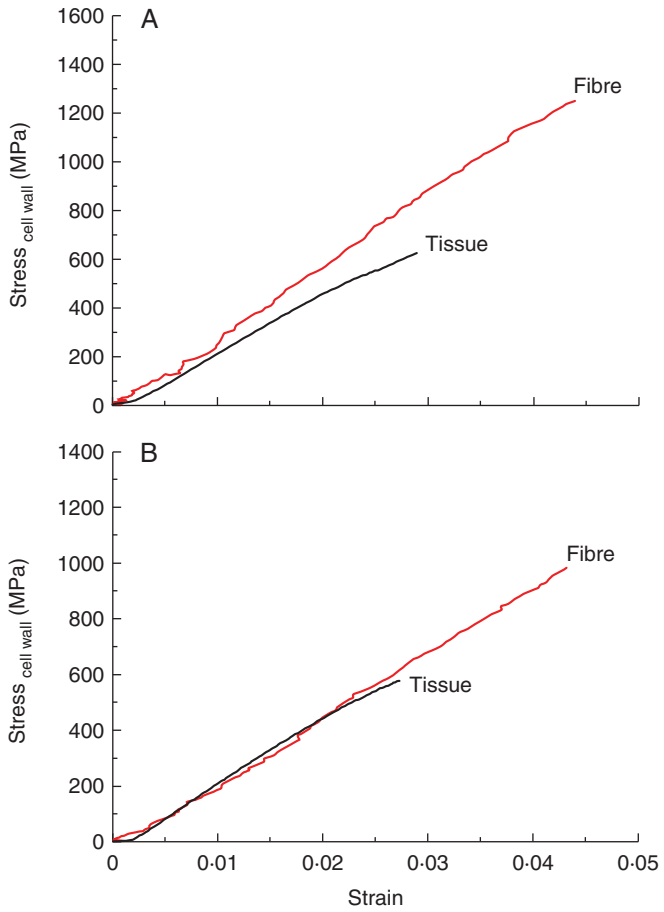

FIG. 8. Representative stress–strain curves of single fibres and fibre bundles of (A) bamboo and (B) spruce latewood calculated on the basis of cell wall cross-sections.

DISCUSSION

This comparison of plant material structure and properties between a monocotyledonous bamboo and a spruce softwood at different hierarchical levels has revealed crucial features with regard to the mechanical performance and material optimization of the two plant systems. In combination with the assumption that the lack of secondary thickening growth in bamboo results in different mechanical exposure of the plant material in comparison with spruce, novel insights regarding material adaptation can be gained.

The tensile tests revealed marked differences in tensile stiffness and strength between bamboo and spruce latewood tissues as well as fibres, but only minor differences in the mechanical properties between the cell walls of the two tissue types (Figs 6 and 7). This suggests that the pronounced differences in the tensile properties of both tissue types and fibres can be attributed to different cell wall cross-sectional areas in a fibre or fibre bundle, rather than to the cell wall itself. This observation and the general stress–strain behaviour are in line with the small MFAs that were measured in the dominating cell wall layers of both tissue types by WAXS and Raman mapping. The orientation of cellulose microfibrils in cell walls is known to dictate the mechanical properties of wood in its axial direction, and almost axially oriented cellulose microfibrils in the cell wall result in a material that is stiff but has low toughness (Cave, 1969; Reiterer *et al.*, 1999).

Bamboo fibres exhibit an essentially round-shaped cell cross-section as opposed to the relatively bigger latewood tracheids, which have a nearly rectangular or hexagonal cell shape. Raman mapping revealed a unique multilayered wall structure with alternating thick and thin layers in bamboo fibres, which is contrary to the typical three-layered secondary wall of wood tracheids, building a sandwich-like structure with a dominating middle layer (S2) (Figs 3 and 4). The Raman spectroscopic analysis also indicated the presence of a large amount of hydroxycinnamic acids (ferulic and *p*-coumaric acids) in the cell walls of bamboo fibres, with especially high levels in the cell corners and the middle lamella (Fig. 5). Hydroxycinnamic acids have been found to cause cross-linkage of cell wall polysaccharides and to contribute to the formation of polysaccharide–lignin complexes, which increase cell wall rigidity and improve the mechanical properties of the wall (Lybeer and Koch, 2005). However, these geometrical and chemical features seem to be of minor relevance or are superimposed when evaluating the contribution of cell–cell interactions to tissue properties. As Fig. 8 illustrates, both bamboo and spruce show the same pattern in the comparison of tissue and fibre properties. Tissues and fibres (calculated on a cell wall basis for comparability) have the same stiffness ($P > 0{\cdot}05$, Mann–Whitney *U*-test) but tissue strength is significantly lower than fibre strength ($P < 0{\cdot}05$). When tissues are stretched to a critical strain level, the fibres are expected to loose contact due to relatively weak intercellular adhesion, resulting in cell–cell debonding and tissue failure. In bamboo fibres the middle lamella appears to be more heavily lignified compared with wood tracheids, probably enhancing the ability to resist shear stresses during straining, whereas the nearly rectangular cell shape of wood tracheids tends to increase the interface area between cells and thus counteracts the effect of the less lignified middle lamella. This suggests that both tissue types break because of failure at the fibre–fibre interface and that both bamboo and spruce can transfer stiffness but not the excellent tensile strength from the fibre to the tissue level.

From this one can conclude that, despite marked differences in the structural features of the cell wall between bamboo fibres and wood tracheids, such as cell shape, thickness and arrangement of cell wall layers, as well as chemical composition, the mechanical properties of the cell wall are predominant and comparable in terms of tensile stiffness and strength, because of the small MFAs in the dominating cell wall layers. In consequence it seems to be simply the greater accumulation of plant cell wall material in fibres and fibre bundles of bamboo that leads to its excellent mechanical performance, which is in accordance with a plant adaptation strategy based on ongoing cell wall formation by living fibres.

However, it should be emphasized that at a higher hierarchical level the interplay between vascular bundles and parenchymatous tissue is also highly relevant (Rüggeberg *et al.*, 2009). Furthermore, only the tensile behaviour could be compared and evaluated using the techniques available in the current study. Bamboos and trees are subjected to bending caused by wind loads and therefore optimization towards compressive stresses also needs to be considered. Bamboo in particular has

to sustain large flexural deformation due to wind loads. Failure is most likely to occur as a result of local buckling of the fibrils in the cell walls on the compression side, leading to the formation of kink bands at the macroscopic level, as frequently observed in the failure mode of wood in compression. From our study, we assume that bamboo might have developed an efficient strategy to cope with the instability of the cell wall under compression. Its thick-walled fibres resemble a solid tube and are stabilized laterally by being glued together by the heavily lignified middle lamella to form stiff fibre caps, which are properly embedded in the compressible parenchymatous tissues. Moreover, the multilayered wall structure of bamboo fibres has been suggested to be able to resist longitudinal compressive stresses by frequent changes in the microfibril angles in the multilamellar cell wall, which provide interfaces that inhibit the lateral propagation of kinks across the cell wall (Murphy and Alvin, 1992).

To conclude, material optimization towards extremely compact fibres with a multilamellar cell wall in bamboo might be a result of a plant growth strategy compensating for the lack of secondary thickening at the material level. This is not only favourable for the biomechanics of the plant, but is also increasingly utilized in terms of engineering products made from bamboo culms.

ACKNOWLEDGEMENTS

This work was financially supported by the FP7: People Marie-Curie action COFUND and the National Natural Science Foundation of China (31170527, 31370563). We thank the Bundesamt für Umwelt (BAFU) and Lignum, Switzerland, for financial support of the Wood Materials Science Group at ETH and Empa. The authors would like to thank the reviewers for their comments, which helped to improve the manuscript.

LITERATURE CITED

Agarwal UP. 1999. An overview of Raman spectroscopy as applied to lignocellulosic materials. In: Argyropoulos DS. ed. *Advances in lignocellulosics characterization*. Atlanta, GA: TAPPI Press, 209–225.

Agarwal UP, Ralph SA. 1997. FT-Raman spectroscopy of wood: identifying contributions of lignin and carbohydrate polymers in the spectrum of black spruce (*Picea mariana*). *Applied Spectroscopy* **51**: 1648–1655.

Amada S, Ichikawa Y, Munekata T, Nagase Y, Shimizu H. 1997. Fiber texture and mechanical graded structure of bamboo. *Composites Part B: Engineering* **28**: 13–20.

Burgert I, Keckes J, Frühmann K, Fratzl P, Tschegg SE. 2002. A comparison of two techniques for wood fibre isolation – evaluation by tensile tests on single fibres with different microfibril angle. *Plant Biology* **4**: 9–12.

Burgert I, Frühmann K, Keckes J, Fratzl P, Tschegg SE. 2003. Microtensile testing of wood fibres combined with video extensometry for efficient strain detection. *Holzforschung* **57**: 661–664.

Burgert I, Eder M, Frühmann K, Keckes J, Fratzl P, Tschegg SE. 2005. Properties of chemically and mechanically isolated fibres of spruce (*Picea abies* [L.] Karst.). Part 3: mechanical characterization. *Holzforschung* **59**: 354–357.

Cave ID. 1969. The longitudinal Young's modulus of *Pinus radiata*. *Wood Science and Technology* **3**: 40–48.

Crow E, Murphy RJ. 2000. Microfibril orientation in differentiating and maturing fibre and parenchyma cell walls in culms of bamboo (*Phyllostachys viridiglaucescens* (Carr.) Riv. & Riv.). *Botanical Journal of the Linnean Society* **134**: 339–359.

Eder M, Rüggeberg M, Burgert I. 2009. A close-up view of the mechanical design of arborescent plants at different levels of hierarchy – requirements and structural solutions. *New Zealand Journal of Forestry Science* **39**: 115–124.

Gierlinger N, Schwanninger M. 2006. Chemical imaging of poplar wood cell walls by confocal Raman microscopy. *Plant Physiology* **140**: 1246–1254.

Gierlinger N, Schwanninger M. 2007. The potential of Raman microscopy and Raman imaging in plant research. *Spectroscopy* **21**: 69–89.

Gierlinger N, Keplinger T, Harrington M. 2012. Imaging of plant cell walls by confocal Raman microscopy. *Nature Protocols* **7**: 1694–1708.

Gritsch CS, Kleist G, Murphy R. 2004. Developmental changes in cell wall structure of phloem fibres of the bamboo *Dendrocalamus asper*. *Annals of Botany* **94**: 497–505.

Li H, Shen S. 2011. The mechanical properties of bamboo and vascular bundles. *Journal of Materials Research* **26**: 2749–2756.

Lichtenegger H, Reiterer A, Tschegg SE, Fratzl P. 1998. Determination of spiral angles of elementary fibrils in the wood cell wall: comparison of small-angle X-ray scattering and wide-angle X-ray diffraction. In: Butterfield BG. ed. *Microfibril angle in wood, Proceedings of the IAWA/IUFRO International Workshop on the Significance of Microfibril Angle to Wood Quality*. Canterbury, New Zealand: University of Canterbury, 140–156.

Lin JX, He XQ, Hu YX, Kuang TY, Ceulemans R. 2002. Lignification and lignin heterogeneity for various age classes of bamboo (*Phyllostachys pubescens*) stems. *Physiologia Plantarum* **114**: 296–302.

Lybeer B, Koch G. 2005. Lignin distribution in the tropical bamboo species *Gigantochloa levis*. *IAWA Journal* **26**: 443–456.

Murphy RJ, Alvin KL. 1992. Variation in fibre wall structure in bamboo. *IAWA Bulletin* **13**: 403–410.

Murphy RJ, Alvin KL. 1997. Fibre maturation in the bamboo *Gigantochloa scortechinii*. *IAWA Journal* **18**: 147–156.

Niklas KJ, Spatz HC. 2012. *Plant physics*. Chicago: The University of Chicago Press.

Obataya E, Kitin P, Yamauchi H. 2007. Bending characteristics of bamboo (*Phyllostachys pubescens*) with respect to its fiber-foam composite structure. *Wood Science and Technology* **41**: 385–400.

Okubo K, Fujii T, Yamamoto Y. 2004. Development of bamboo-based polymer composites and their mechanical properties. *Composites Part A: Applied Science and Manufacturing* **35**: 377–383.

Osorio L, Trujillo E, Van Vuure AW, Verpoest I. 2011. Morphological aspects and mechanical properties of single bamboo fibers and flexural characterization of bamboo/epoxy composites. *Journal of Reinforced Plastics and Composites* **30**: 396–408.

Parameswaran N, Liese W. 1976. On the fine structure of bamboo fibres. *Wood Science and Technology* **10**: 231–246.

Parameswaran N, Liese W. 1980. Ultrastructural aspects of bamboo cells. *Cellulose Chemistry and Technology* **14**: 587–609.

Perera PN, Schmidt M, Chiang VL, Schuck PJ, Adams PD. 2012. Raman-spectroscopy-based noninvasive microanalysis of native lignin structure. *Analytical and Bioanalytical Chemistry* **402**: 983–987.

Ram MS, Dowell FE, Seitz LM. 2003. FT-Raman spectra of unsoaked and NaOH-soaked wheat kernels, bran, and ferulic acid. *Cereal Chemistry* **80**: 188–192.

Reiterer A, Lichtenegger H, Tschegg SE, Fratzl P. 1999. Experimental evidence for a mechanical function of the cellulose microfibril angle in wood cell walls. *Philosophical Magazine A* **79**: 2173–2184.

Rüggeberg M, Speck T, Burgert I. 2009. Structure-function relationships of different vascular bundle types in the stem of the Mexican fanpalm (*Washingtonia robusta*). *New Phytologist* **182**: 443–450.

Shao Z, Fang C, Huang S, Tian G. 2010. Tensile properties of moso bamboo (*Phyllostachys pubescens*) and its components with respect to its fiber-reinforced composite structure. *Wood Science and Technology* **44**: 655–666.

Speck T, Burgert I. 2011. Plant stems: functional design and mechanics. *Annual Review of Materials Research* **41**: 169–193.

Sun L, Varanasi P, Yang F, Loqué D, Simmons BA, Singh S. 2012. Rapid determination of syringyl: guaiacyl ratios using FT-Raman spectroscopy. *Biotechnology and Bioengineering* **109**: 647–656.

Takei T, Kato N, Iijima T, Higaki M. 1995. Raman spectroscopic analysis of wood and bamboo lignin. *Mokuzai Gakkaishi* **41**: 229–236.

Wang X, Ren H, Zhang B, Fei B, Burgert I. 2012. Cell wall structure and formation of maturing fibres of moso bamboo (*Phyllostachys pubescens*) increase buckling resistance. *Journal of the Royal Society Interface* **9**: 988–996.

Yu Y, Tian G, Wang K, Fei B, Wang G. 2011. Mechanical characterization of single bamboo fibers with nanoindentation and microtensile technique. *Holzforschung* **65**: 113–119.